Supporting Information For

Bio-Functional, Lanthanide-Labeled Polymer Particles by Seeded Emulsion Polymerization and their Characterization by Novel ICP-MS Detection

Stuart C. Thickett,[a] Ahmed I. Abdelrahman,[a] Olga Ornatsky,[a] Dmitry Bandura,[a] Vladimir Baranov[a] and Mitchell A. Winnik[a*]

Received (in XXX, XXX) Xth XXXXXXXXX 200X, Accepted Xth XXXXXXXXX 200X
First published on the web Xth XXXXXXXXX 200X
DOI: 10.1039/b000000x

.

Theory of Targeted Lanthanide Loading

We proposed to use seeded emulsion polymerization to create Ln-tagged particles with a known concentration of loaded metal. A series of steps were needed to determine the mass of Ln complex to obtain a chosen number of Ln ions per particle in a sample. The procedure used to determine the relevant quantities of second-stage monomer, lanthanide complex, added surfactant etc. is described below.

Determination of Particle Number density (N_p)

The number of particles per unit volume (L^{-1}) can be readily calculated from the following expression:[1]

$$N_p = \frac{m_p^0}{\frac{4}{3}\pi r^3 d_p} \qquad \text{(SI.1)}$$

Where m_p^0 is the solids content of the latex in question (g L^{-1}), r the average particle radius and d_p is the density of the polymer.

Determination of Saturation Monomer Concentration C_p^{sat}

When polymer particles are swollen with additional monomer, there is a saturation limit where no further monomer can be accommodated into the particle phase. We aimed to remain below the saturation limit for particle swelling, so that the added monomer is located within the seed particles and not in additional droplets.

The saturation monomer concentration (C_p^{sat}) is often experimentally determined by the 'static swelling' method[1] however theoretical values of this concentration can also be easily estimated through the Morton equation.[2] The Morton equation predicts the equilibrium volume ratios of a polymer/monomer mixture in the interior of polymer particles. Limitations exist in the use of this equation as there are parameters that are either poorly known or difficult to measure, however typically the saturation monomer concentration can be estimated to within 10 % of the actual value. The Morton Equation is presented here:

$$\ln(1-\phi_p) + \phi_p + \chi\phi_p^2 + \frac{2\Gamma V_{sM}}{r\,RT}\phi_p^{1/3} = 0 \qquad \text{(SI.2)}$$

where χ is the Flory-Huggins Interaction parameter, Γ the interfacial tension of latex particles, V_{sM} the partial molar volume of the monomer (= M_0/d_M where M_0 is the molecular weight and d_M the density of monomer) and ϕ_p is the volume fraction of polymer per particle. For a given r (particle radius), the Morton Equation can be solved iteratively to yield ϕ_p and hence C_p^{sat} (= $(1-\phi_p)/V_{sM}$).

Determination of Mass of Monomer Added to Latex

Knowledge of r and C_p^{sat} allowed the final particle size after swelling with monomer to be calculated. From this final particle size, the amount of monomer that can be added to the latex (while remaining below the saturation limit) was determined. The swollen particle size r_s is related to r and C_p^{sat} through the following relation:

$$\frac{r_s}{r} = \left(\frac{C_p^{sat}}{C_p^{sat} - d_M M_0}\right)^{1/3} \qquad \text{(SI.3)}$$

where d_M is the density of monomer. The weight fraction of polymer per particle w_p was calculated (this is different to the volume fraction per particle), and is given by:

$$w_p = \frac{d_p}{d_p + \frac{C_p^{sat} M_0}{1 - C_p^{sat}\frac{M_0}{d_M}}} \qquad \text{(SI.4)}$$

Once w_p was calculated, the mass of monomer m_{MON} that can be incorporated was determined for a given mass of latex. (as $w_M = 1 - w_p$).

Lanthanide Loading

Once a target (T_{Ln}) number of lanthanide ions per particle was chosen (e.g. 10^6 per particle), the mass of Ln complex required was calculated. The number concentration of lanthanide ions per unit volume of latex is $T_{Ln}N_p$, and the mass of lanthanide complex needed per unit volume is $T_{Ln}N_pM_{Ln}/N_A$ where M_{Ln} is the molecular weight of the

lanthanide complex and N_A is Avogadro's number.

Surfactant-Free Emulsion Polymerization (SFEP) Experimental Optimization

In this section the experimental results of SFEP syntheses using the acid-functional initiator ACVA are presented. Different reaction parameters were varied and the final particle size and polydispersity of the PSD of the resulting particles were determined.

Dependence on Reaction Temperature

The final particle size and morphology of particles synthesized by SFEP was studied as a function of reaction temperature at constant ionic strength. Ionic strength was regulated by addition of NaCl. Additionally, two molar equivalents of NaOH were added per mole of ACVA. The [ACVA] concentration was held constant at 2.4 mM.

Table S1. PSD Data for SFEP/ACVA Latexes as a function of polymerization temperature

Sample Name	Temp (K)	Ionic strength (mM)	D_n (nm)	CV_D (%)	Comments
st039	333	51.0	*No latex formed*		
st068	343	40.3	305	3.8	Some larger particles
st040	353	51.6	528	1.7	Very monodisperse

At 333 K, no latex was formed several hours after the addition of initiator to the pre-emulsion. In sample st068, which was performed at 343 K, a latex formed readily and was quite monodisperse when analyzed by SEM, however some larger particles were present (see Figure S1A). Experiment st040 (synthesized at 353 K, Figure S1B) has been discussed in the manuscript and was shown to have a particularly narrow PSD. The variation in average size (305 nm versus 528 nm) is not related to the final fractional conversion as st068 has a final particle number N_p of the order of 4 times larger than st040.

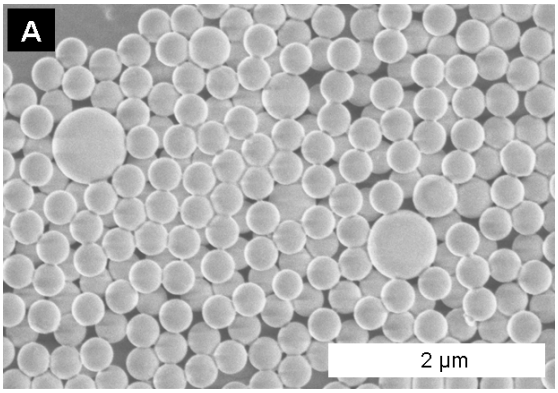

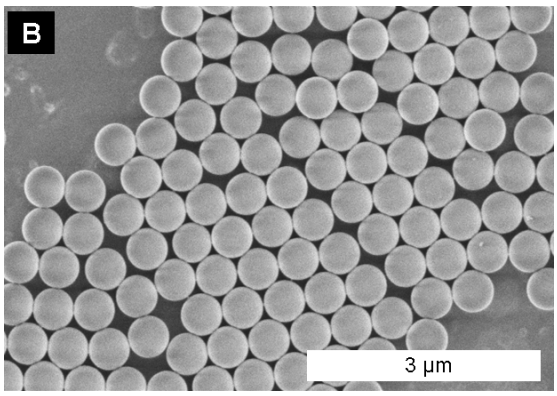

Fig. S1. SEM images of SFEP latexes synthesized as a function of reaction temperature. (A) st068 polymerized at 343 K; (B) st040 polymerized at 353 K.

Influence of Ionic Strength at Constant Temperature

The effect of varying the ionic strength of the aqueous phase in SFEP syntheses was investigated at 353 K. This temperature was chosen as the results described previously suggest that the PSD is significantly narrower at high temperatures. The [ACVA] concentration was again 2.4 mM; results are presented in Table S2.

Table S2. Influence of ionic strength on the final PSD of SFEP latexes synthesized with ACVA at 353 K.

Sample Name	Temp (K)	Ionic strength (mM)	D_n (nm)	CV_D (%)	Comments
st040	353	51.6	528	1.7	Very monodisperse
st067	353	23	162	12.3	Some very large particles

The reduction in particle size observed at lower ionic strength was over 350 nm. The distribution of these small particles was quite broad and the sample contained some extremely large particles, of the order of several microns in size. An SEM images of st067 is shown in Figure S2. It would appear that SFEP systems initiated by ACVA are strongly dependent on ionic strength.

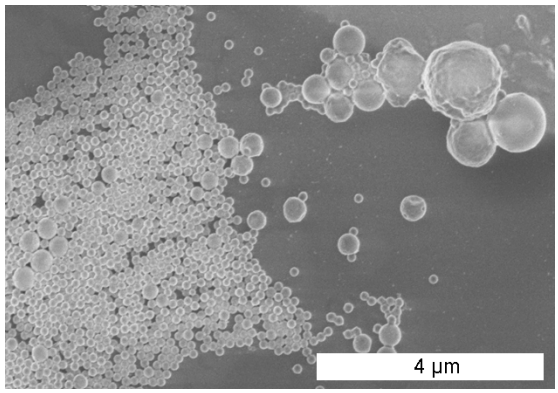

Fig. S2. SEM image of SFEP latex st067 polymerized at high reacton temperature (353 K) and low ionic strength (23 mM).

We infer that particle synthesis by SFEP using ACVA is particularly sensitive to variations in reaction conditions, such as temperature and ionic strength. Under some conditions, multimodal PSDs or broad PSDs were generated. The best conditions were those of high temperature and high ionic strength, where monodisperse particles of size approximately 500 nm (such as st040) were formed.

Replicate experiments were performed to determine the reproducibility of particle synthesis under conditions of high ionic strength and high temperature. These conditions were identical to those used for the synthesis of st040. The conditions were the following: polymerization temperature 353 K, ionic strength approximately 50 mM. (through addition of NaCl), [ACVA] = 3.5 mM, polymerization time 24 hours, equimolar amount of base added to neutralize ACVA, overhead stirring at 200 rpm. All final conversions were low as previously observed (typically 25 %). This low conversion was attributed to rapid consumption of the initiator at this temperature.[3] The results are presented in Table S3.

Table S3. PSD Data for replicate experiments in the synthesis of ACVA-stabilized latexes by SFEP under conditions of high ionic strength and high temperature.

Sample	[Ionic strength] (mM)	D_n (nm)	CV_D (%)	N_p (L^{-1})
st040	52	528	1.7	2.4×10^{14}
st098	48	1466	5.8	4.7×10^{12}
st100	48	303	2.8	1.4×10^{15}
st102	46	*No latex observed*		

The variability in particle size was very high in these experiments. It is hard to explain the absence of any meaningful particle formation for st102 – the final solids was close to zero and no latex particles were observed. In the cases of st040 and st100, monodisperse particles were synthesized, however the difference in size was close to a factor of 2.

It was postulated that the pH of the continuous phase is particularly important in SFEP when ACVA is used as the initiator. The solubility of ACVA in water in its protonated form is very poor. The base (NaOH) was only added to the initiator solution in order to assist dissolution, however the pre-emulsion contained no added base. The next section discusses the use of an aqueous-phase buffer in the SFEP step.

SFEP in Buffered Media

Sodium hydrogencarbonate ($NaHCO_3$) was used to buffer the aqueous phase in new SFEP experiments at high reaction temperatures (353 K). $NaHCO_3$ regulated the ionic strength in these experiments as opposed to the 'inert' NaCl. It was postulated that effective dissolution of the initiator occur in the presence of the buffer, allowing for greater experimental reproducibility. A lower total ionic strength (approximately 25 mM) was chosen to avoid potential coagulation. The polymerization temperature was 353 K. The results of these syntheses are presented in Table S4 and Figure S3.

Table S4. PSD Data of SFEP latexes synthesized with ACVA in the bicarbonate-buffered media at 353 K.

Sample Name	[ACVA] (mM)	Ionic strength (mM)	D_n (nm)	CV_D (%)
st153	2.0	24.1	555	1.6
st165	2.0	22.8	612	2.1
st168	1.9	23.1	701	1.9

The three syntheses performed in the presence of $NaHCO_3$ buffer yielded monodisperse latexes with regular morphologies and no secondary nucleation. There was good consistency in the final particle size, much moreso than what was observed in previous experiments in the absence of buffer. The final conversion was also moderately high – between 70 to 85 % for the three samples; previous fractional conversions (in systems where ionic strength was regulated by NaCl) were of the order of 25-30 %.

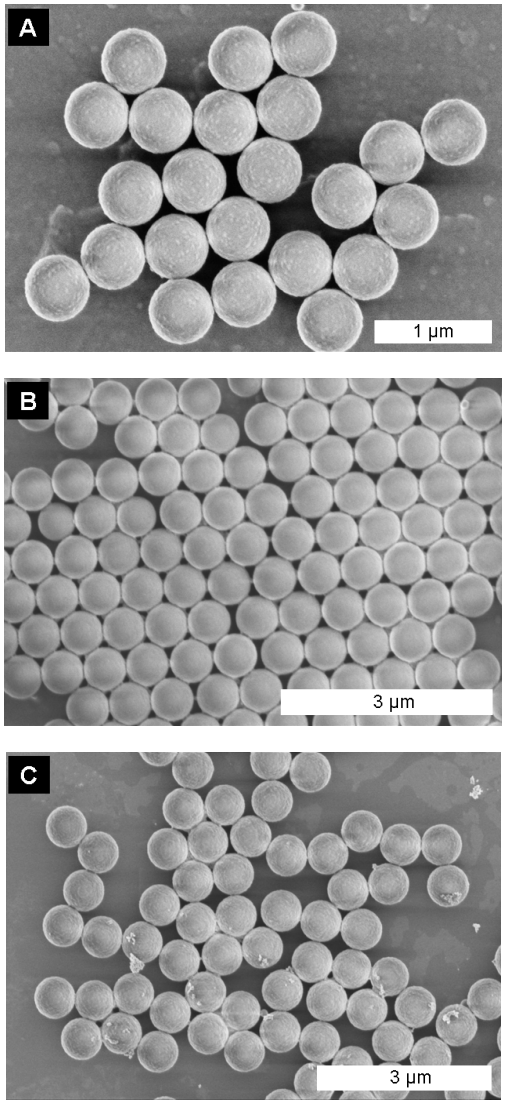

Fig. S3. SEM images of three replicate SFEP latexes synthesized with ACVA as initiator in the presence of buffered media. (A) st153; (B) st165; (C) st168.

Surface Acid Titration Data

Surface acid titration experiments were performed to determine the number of accessible carboxylic acid groups on the surface of our particles. Two different sets of particles were analyzed – the seed latex st040 and the latex ST077, which was the resultant latex from seeded emulsion polymerization using st040 as a seed (Method 1 polymerization).

All experiments were performed as back titrations. For most analyses, the latex sample was diluted to 0.05 % w/w and 200 µL of 0.1 M NaOH was added to the latex to deprotonate any surface acid groups and provide an excess of base. Titration was performed through addition of 0.01 M HCl. Other methods were also used, such as titration with 0.1 M HCl, titration of a more concentrated latex solution (1:10 dilution in water) and titration after redispersion into 25 mM NaCl. The pH of the resultant solution was monitored in all cases, and the conductivity of the solution in some cases, in accordance with the protocol developed by Kawaguchi *et al*.[4] The use of a 'blank' solution (to account for dissolved CO_2) provided a reference point to determine the number of acid groups attributed to each particle.

Sample st040

A representative titration curve (for the titration of st040) is shown in Figure S4. Two distinct equivalence points are present; the first at pH 7.1 and the second slightly above pH 4. The volume difference between the two equvalence points was used to calculate the number of acid groups on the particle surface. These calculations (for all methods used) are presented in Table S5.

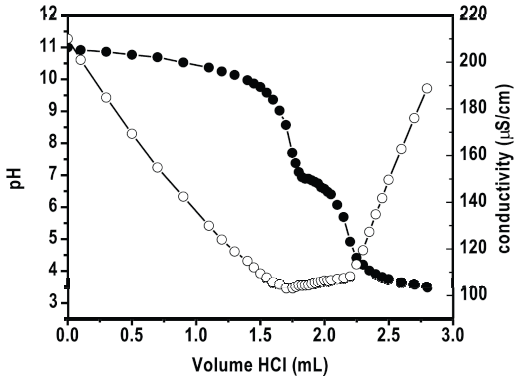

Fig. S4. Surface acid titration of st040 (diluted to 0.05 % w/w solids) with 0.01 M HCl (measurement by pH and conductivity).

Table S5. Surface acid titration data for seed latex st040 as determined by a variety of different measurements. 'pH 1' corresponds to the pH at the first inflection point observed; 'pH 2' corresponds to the second inflection point.

Method	pH 1	pH 2	µmol acid (expected)	µmol acid (measured)	Groups per particle (× 10^7)
1:10 dilution in water	7.05	4.17	3.5	2.6	0.82
Excess dilution, conc. acid, conductivity	7.48	3.99	4.3	4.7	1.2
Excess dilution, weak acid, conductivity	7.7	4.9	1.6	2.8	1.95

The results in Table S5 indicate that a significant number (approximately 10^7 per particle) of acid groups are present on the surface of these latexes. Typically, more surface acid groups were detected than what should be theoretically present in the latex (based on the experimental formulation). The error in the method is approximately 20 %. It was postulated that hydrolysis of the cyano group on the initiator fragment may also produce additional carboxylic acid groups that can be detected by titration.

Sample ST077

Sample ST077 represents the seeded growth of latex st040 with a monomer/lanthanide mixture with initiation by KPS ('Method 1' polymerization). The results for back-titrations of this latex are tabulated below. After seeded growth, we infer that the measured number of surface acid groups (per particle) is unchanged when compared to seed latex st040.

Table S6. Surface acid titration data for latex ST077 as titrated by a variety of different methods. 'pH 1' corresponds to the pH at the first inflection point observed; 'pH 2' corresponds to the second inflection point.

Method	pH 1	pH 2	µmol acid (expected)	µmol acid (measured)	Groups per particle (× 10^7)
1:10 dilution in water	7.2	4.5	1.6	2.2	1.22
1:10 dilution in 25 mM NaCl	8.2	5.0	1.3	1.0	0.68
Excess dilution, weak acid, conductivity	6.8	4.6	1.3	1.0	0.71

The Role of Cyclodextrin

In the manuscript, we discussed the impact that addition of a member of the cyclodextrin family had on the particle growth process during seeded emulsion polymerization. Initial experiments where seeds were swollen with a mixture of monomer and dissolved Ln complex demonstrated extensive amounts of secondary nucleation. The addition of methyl-β-cyclodextrin (in a molar excess relative to the Ln complex) had the effect of significantly reducing the amount of small particles observed by SEM. The particle size distributions (PSDs) that correspond to the two syntheses reported in the manuscript are shown in Figure S5. The value of Φ_{NEW} (the volume fraction of polymer corresponding to the 'new'

particle population due to secondary nucleation) was calculated for the two PSDs shown in Figure S5. Φ_{NEW} decreases from 0.67 in the absence of cyclodextrin to 0.02 in the presence of cyclodextrin. This is a decrease in Φ_{NEW} by a factor of approximately 33.

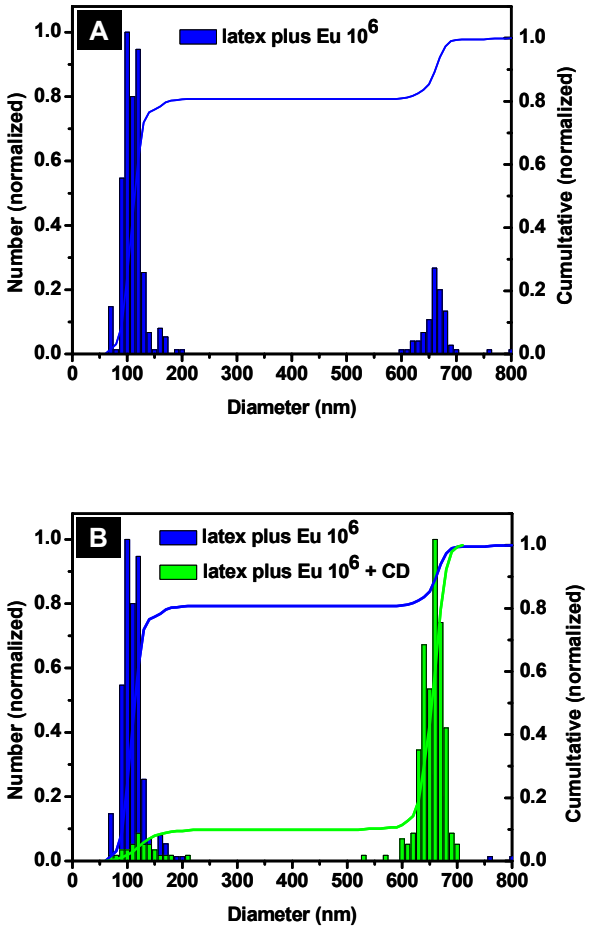

Fig. S5. Particle Size Distributions for the Method 1 seeded emulsion polymerization of st040 (as reported in the manuscript) in the absence (A) and presence (B) of methyl-β-cyclodextrin. The blue and green lines correspond to the cumulative distribution of the PSD (right axis).

Sulfate-Stabilized Latex

A PS latex was synthesized by SFEP with KPS as the initiator, which was denoted st109. The latex was monodisperse (D_n = 621 nm, CV_D = 4.4 %) and of sufficient size for seeded emulsion polymerization performed by Method 2 (where a sulfate-stabilized seed is further polymerized with ACVA). An SEM image and the determined number PSD for st109 is shown in Figure S6.

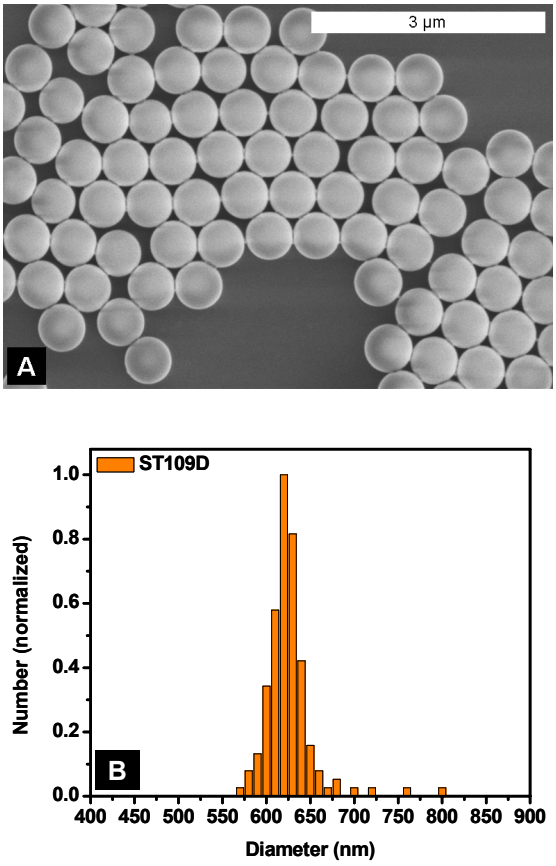

Fig. S6. (A) SEM image and (B) number PSD for sulfate-stabilized latex st109.

EDX Linescans

EDX linescans were performed across particles from sample ST077 (see Figure S7). Figure S7B gives the count profile for both carbon and europium as a function of linescan distance. The profile for both elements showed the same qualitative shape (albeit at different intensities). These profiles are typical for incorporation into a spherically shaped object. From this result we inferred that the Eu is incorporated within the interior of the PS particles when synthesized by this method.

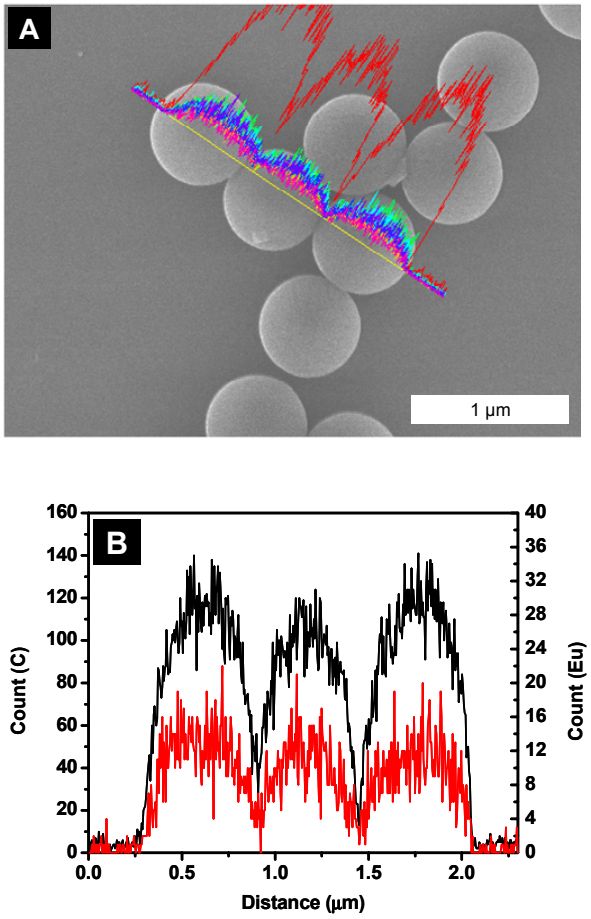

Fig. S7. (A) EDX linescan image of particles from sample ST077. The red curve corresponds to the Carbon count over the yellow line scanned across the three particles. The pink line corresponds to the Europium profile. (B) EDX count profiles from Image A as a function of distance (measured left to right). Black profile – Carbon distribution; Red profile – Europium distribution.

Lanthanide Leaching Data

In the manuscript, we discussed that Ln leaching from the particle interior was studied under three different sets of conditions. Two of these experiments were time-depenedent leaching experiments where the Ln concentration in the supernatant was monitored as a function of time. One experiment was performed in a pH 5.2 buffer to mimic bioconjugation conditions, and the other was performed in the presence of a strong metal chelating agent (DTPA) dissolved in the aqueous phase.

We present the leaching data for experiments performed in the presence of a DTPA solution. In the manuscript we report that the concentration of leached Eu from particles from sample ST141 was low (2.6 – 2.8 ppb) and approximately constant over time. The measured Eu concentration as a function of time by ICP-MS is shown in Figure S8. The results, as interpreted in the manuscript, suggest that there is no continual leaching of Ln into the aqueous phase as a function of time.

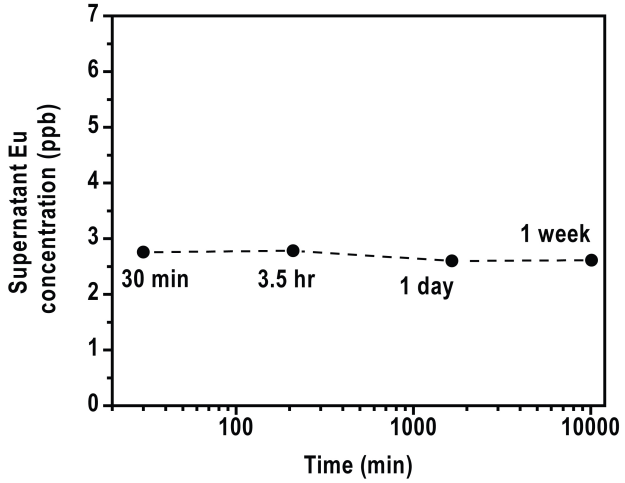

Fig. S8. Eu concentration (measured by ICP-MS) in the supernatant of sample ST141 as a function of time during exposure to a 1 mM DTPA solution pH 3.2. The particles were synthesized at an Eu concentration of 630 ppm.

Average Ln per Particle and CV_{Ln} Values

The experimentally determined Ln per particle (calculated by mass cytometry analysis) and the coefficients of variation (CV_{Ln}) of the Ln content distributions (LnCDs) discussed in the manuscript are listed in Table S7. The agreement between the experimental and theoretical Ln loading per particle was discussed in the manuscript. The CV_{Ln} values reported here are typically greater than 20 %.

Table S7. Coefficient of variation of LnCD (CV_{Ln}) as determined from CyTOF analyses for particles synthesized by seeded emulsion polymerization. Unless otherwise specified, the loaded metal is Eu

Sample	Method	Average Ln per particle (CyTOF)	CV_{Ln} (%)
ST073	1	2.72×10^7	19.5
ST077	1	2.02×10^6	19.2
ST162	1	6.59×10^6	29
ST167	1	2.4×10^6 (Ho)	30
ST120	2	1.56×10^7	16.1
ST124	2	1.6×10^7	44.1
ST125	2	1.19×10^7 (Tb)	18.2
ST130	2	1.11×10^7 (Eu)	26
		1.35×10^7 (Tb)	21
ST141	2	1.29×10^7	21
ST154	2	1.33×10^7	32[a]

[a] ST154 performed with 10-fold reduction in initiator (ACVA) concentration

Two-Dimensional Mass Cytometry Data

An example of two-dimensional mass cytometry output is shown in Figure S9. This figure demonstrates the detection of three individual Eu-tagged particles from sample ST077 (shown in the red circle). The horizontal axis in this figure is the time-of-flight (TOF) axis, which allows for differentiation of multiple Ln ions. The vertical axis is equivalent to the time axis, as many mass spectra are recorded per second to allow for quantification of the number of lanthanide ions detected per particle event.

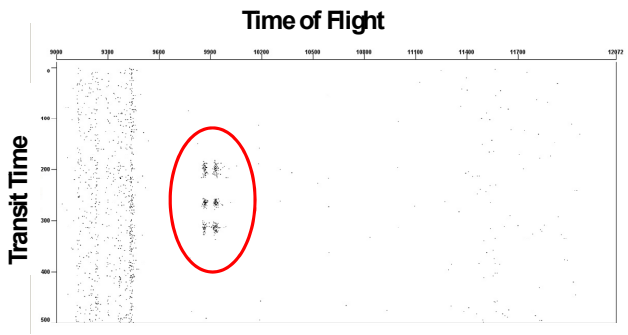

Fig. S9. Raw two-dimensional mass cytometry data from the analysis of sample ST077 (loaded with Eu at a concentration of approximately 10^6 ions per particle). Circled in red is the data from the transit of three particles through the instrument. Each particle gives two signals on the TOF axis due to Eu consisting of two dominant isotopes in approximately equal abundance.

Ln Content Distributions

The Ln content distributions (LnCDs) of the majority of samples reported in Table S7 are shown below in the following Figures. Data for sample ST162 was shown in the manuscript. If the particles were synthesized in the presence of $Eu(TNB)_3$, an isotopic 'dot-plot' is presented. These dot-plots show the distribution of both Eu isotopes from particle to particle. Some samples were synthesized in the presence of $Ho(TNB)_3$ or $Tb(TNB)_3$, and these Ln ions are monoisotopic. For the monoisotopic lanthanides, a one-dimensional distribution is presented. The numbers on each figure correspond to the fraction of the total particle population that falls within the circled regions presented.

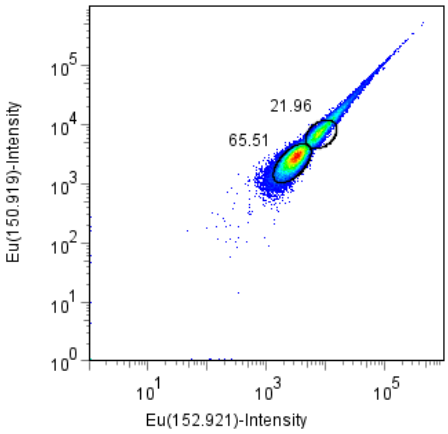

Fig. S10. Eu isotopic dot-plot for sample ST120 (particles synthesized by Method 2 polymerization for Eu loading with targeted value of 1.15×10^7 per particle) as measured by mass cytometry.

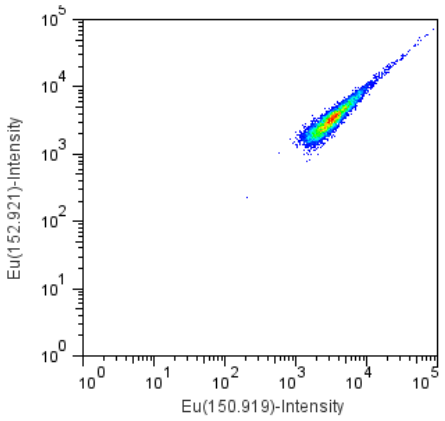

Fig. S11. Eu isotopic dot-plot for sample ST124 (particles synthesized by Method 2 polymerization for Eu loading with targeted value of 1.17×10^7 per particle) as measured by mass cytometry.

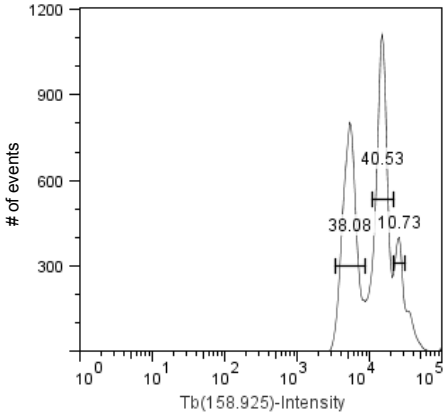

Fig. S12. Tb content distribution for sample ST125 (synthesized by Method 2 polymerization for Tb loading with targeted value of 1.24×10^7 per particle) as measured by mass cytometry.

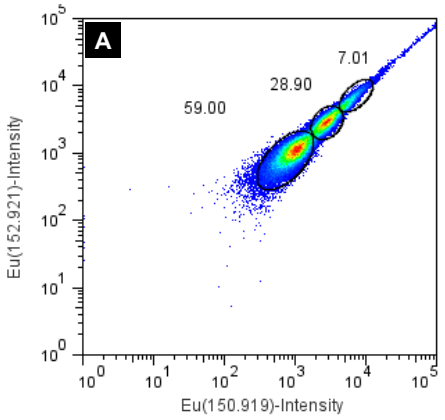

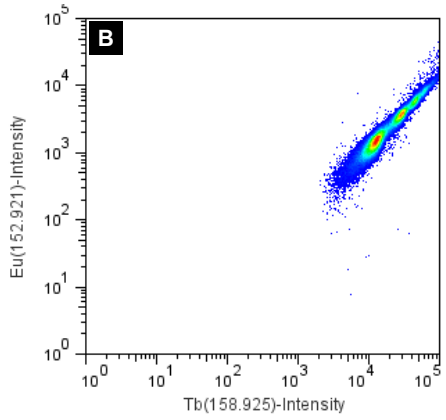

Fig. S13. (A) Eu isotopic dot-plot and (B) ^{153}Eu-Tb isotopic dot-plot for sample ST130 (particles synthesized by Method 2 polymerization for Eu and Tb loading with targeted value of 1.07×10^7 (Eu) and 1.04×10^7 (Tb) per particle) as measured by mass cytometry.

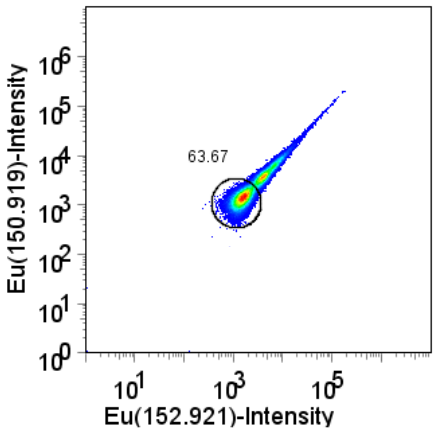

Fig. S14. Eu isotopic dot-plot for sample ST141 (synthesized by Method 2 polymerization for Eu loading with targeted value of 1.06×10^7 per particle) as measured by mass cytometry.

Table of Peak Intensity Data

The LnCDs shown in the previous section typically consist of two (or more) dominant populations. In the isotopic dot-plots, this is evident by the appearance of two or more 'red spots' indicating a high population of particles. Some distributions, such Figure S13 for sample ST130, have three dominant populations of particles.

The mean intensity of all peaks seen in these LnCDs are presented in Table S8. The 'peak ratio,' which corresponds to the ratio of the mean intensity of Peak 2 to Peak 1 (or in some cases Peak 3 to Peak 1) is also provided. For most samples, the peak ratio of Peak 2 to Peak 1 is close to 2. This peak ratio is approximately constant regardless of the isotope chosen for analysis (i.e. ^{151}Eu or ^{153}Eu). The size of this ratio suggests that Peak 2 corresponds to the detection of two particles simultaneously by mass cytometry. LnCDs that demonstrate a third peak (ST125 and ST130) have a peak ratio of Peak 3 to Peak 1 that is between 4 – 5. This possibly corresponds to the detection of many particles at the same time.

Table S8. Peak intensity data from isotopic dot-dot diagrams measured by mass cytometry for Ln-tagged PS particles synthesized by seeded emulsion polymerization. Presented are the peak intensity values for all significant populations detected by the instrument, and the percentage (of the total number of particle events) of the population represented in each peak.

Sample	Element	Peak 1 Intensity	Peak 2 Intensity	Peak Ratio	Peak Percentages (of Total Population)
ST162	^{153}Eu	1413	3199	2.3	46; 28
ST120	^{153}Eu	2735	6798	2.5	68; 27
ST124	^{153}Eu	3263	n/a		One peak only
ST125	^{159}Tb	5131	14189	2.8	38; 41; 11
			23671[a]	4.6[b]	
ST130	^{153}Eu	1493	3849	2.6	59; 29; 7
			7785[a]	5.2[b]	
ST130	^{159}Tb	11600	27300	2.3	59; 29; 7
			51531[a]	4.4[b]	
ST141	^{153}Eu	1576	3015	1.9	63; 27

[a] Intensity of third peak in relevant LnCD; [b] Ratio of Peak 3 to Peak 1

Dynamic Light Scattering Data

The detection of multiple populations in the analysis of our metal labeled particles by mass cytometry was attributed to particle aggregation in solution. The existence of two (or more) aggregated particles may result in multiple particles passing through the mass cytometer at the same time. This hypothesis was investigated through the analysis of our samples by dynamic light scattering (DLS). The details of our DLS analyses are presented in the Experimental section of the manuscript.

Initially, we analyzed the three seed latexes used in this work by DLS. Two of these latexes (st040 and st153) were synthesized by surfactant-free emulsion polymerization (SFEP) using an acid-functional initiator; the other latex (st109) was synthesized using potassium persulfate, which produces particles stabilized by surface sulfate groups. All three latexes were particularly monodisperse (determined from particle size distribution data from numerous SEM images). The correlation functions from DLS measurements for these three latexes is shown in Figure S15 and hydrodynamic diameter values are presented in Table S9. The values of the measured hydrodynamic diameters of our three latexes are in excellent agreement with SEM data, and the nature of the correlation functions indicate a monodisperse PSD free of any aggregation.

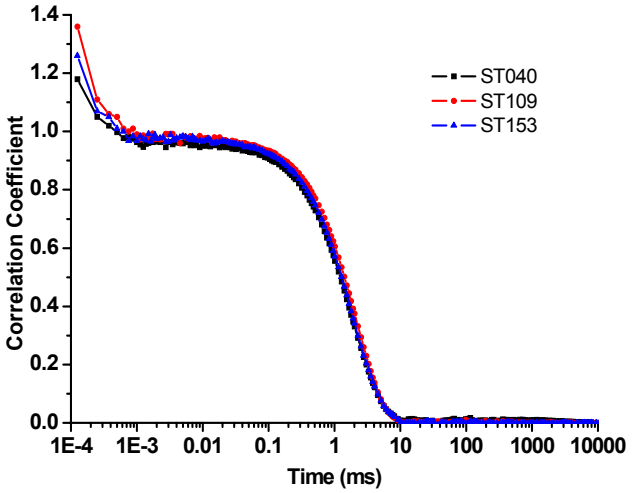

Fig. S15. Correlation functions from DLS for the three seed latexes used in this work. Shown are: st109(black curve, acid-stabilized latex), st109 (red curve, sulfate-stabilized latex) and st153 (blue curve, acid-stabilized latex).

Table S9. Hydrodynamic diameter and polydispersity data from DLS measurements of seed latexes used in this work. Number-average particle diameters obtained from SEM are also provided for comparative purposes.

Seed Latex	Surface group	Hydrodyamic Diameter (D_h, nm)	PDI (DLS)[a]	D_n (nm) from SEM
st040	acid	540	0.13	528
st153	acid	570	0.07	555
st109	sulfate	655	0.07	621

[a] DLS polydispersity index obtained by the second order cumulant analysis[5]

Our next DLS analyses involved studying the solution behaviour of particles after seeded growth and loading of lanthanide ions. In the manuscript, we presented mass cytometry data for sample ST162, which involved the swelling and particle growth of sample st153 and loading of Eu ions at a concentration of approximately 10^7 per particle. Upon analysis of the particles by SEM after polymerization, the particles had grown to a diameter of 821 nm with only a small amount of secondary nucleation (< 5 % with respect to the seed particle volume). The mass cytometry data for ST162 however was strongly bimodal, as were the results for many other particles synthesized as part of this work.

The suggestion that this bimodal (and often multimodal) behaviour was due to particle aggregation was supported by DLS data, such as the correlation functions shown in Figure S16. The long 'tails' in the DLS correlation functions of the two latexes after seeded growth (ST162 and ST167, shown in red and blue respectively) indicate the existence of higher order aggregates in solution. This aggregation behaviour was seen to varying extents in all samples analyzed by DLS. The nature of the correlation functions from these samples also yielded very large DLS polydispersity indices, much greater than the narrow distributions measured by SEM. Poor correspondence was observed between the particle size as measured by SEM compared to light scattering results, sometimes by several hundred nanometres. This data is presented in Table S10.

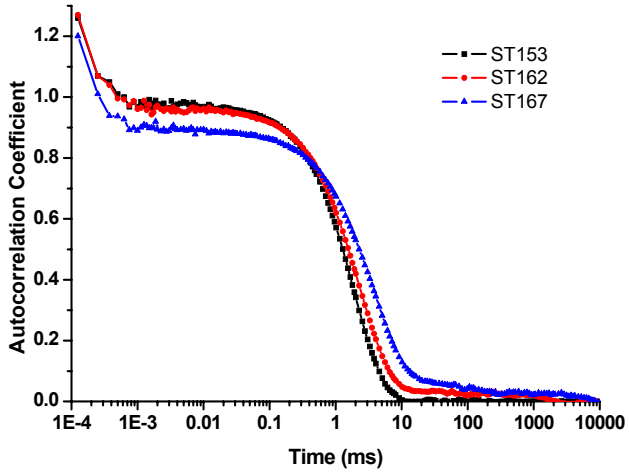

Fig. S16. Correlation functions from DLS for the seed latex st153 (black curve) and particles after seeded growth and lanthanide loading (ST162, red curve and ST167, blue curve).

Table S10. Hydrodynamic diameter and polydispersity data from DLS measurements of latexes after seeded growth. Number-average particle diameters obtained from SEM are also provided for comparative purposes.

Latex	Grown from seed	Hydrodyamic Diameter (D_h, nm)	PDI (DLS)[a]	D_n (nm) from SEM
ST077	st040	600	0.25	650
ST162	st153	566	0.31	821
ST167	st153	822	0.43	744
ST124	st109	640	0.32	771
ST125	st109	596	0.55	726
ST130	st109	520	0.34	854
ST141	st109	420	0.29	759

[a] DLS polydispersity index obtained by the second order cumulant analysis[5]

Bioconjugation Data

In the manuscript, we evaluated the ability of Neutravidin to be covalently attached to the surface of Ln-tagged particles synthesized by seeded emulsion polymerization. The results presented in the manuscript were for one specific sample (ST073). Sample ST073 was prepared by 'Method 1' polymerization to synthesize particles loaded with Eu at approximately 10^7 ions per particle. We used Neutravidin that was pre-labeled with a Tm-containing metal chelating polymer (MCP) and conjugated the labeled Neutravidin to the surface of the particles using EDC as a coupling agent. The sample was then analyzed by mass cytometry.

We present here the bioconjugation results for other Ln-tagged particles synthesized in this work. In particular, we were interested in evaluating the ability of particles synthesized by Method 2 polymerization to undergo bioconjugation. The mass cytometry results of the bioconjugation to four samples (ST120, ST124, ST125 and ST130) synthesized by Method 2 is presented below. In these experiments, a pre-labeled Neutravidin was not used. We attached unlabeled Neutravidin to the particle surface with EDC as a coupling agent and then incubated the sample with an Lu-tagged biotin reporter (a small peptide with one biotin molecule attached at one end and DTPA-Lu at the other end

(Lu-DTPA-Asp-Leu-Leu-Val-Tyr-Asp-Lys(biotin)-amide, MW 1783.1 g/mol, synthesized at The University of Toronto). The strong interaction between biotin and Neutravidin and the presence of the Lu reporter tag allows the bioconjugation process to be studied by mass cytometry. Isotopic dot-dot diagrams and Lu content distributions are presented.

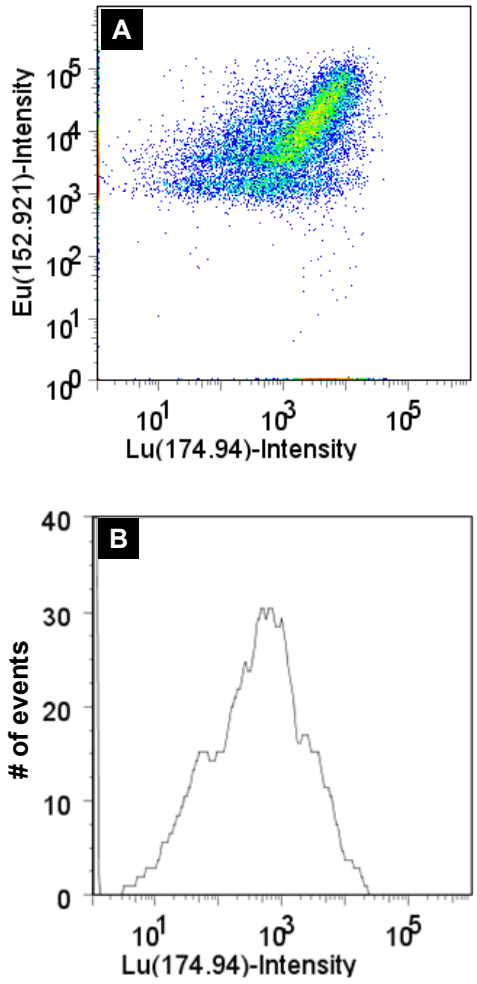

Fig. S17. (A) ^{153}Eu-^{175}Lu isotopic dot-dot diagram for particles from sample ST120 after bioconjugation with Neutravidin and incubation with an Lu-labeled biotin reporter molecule; (B) ^{175}Lu content distribution presented as a one-dimensional projection.

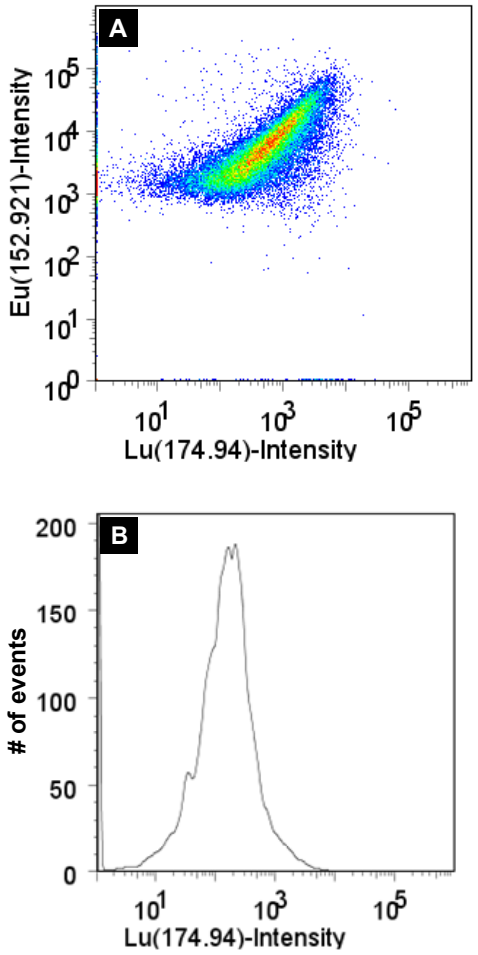

Fig. S18. (A) ^{153}Eu-^{175}Lu isotopic dot-dot diagram for particles from sample ST124 after bioconjugation with Neutravidin and incubation with an Lu-labeled biotin reporter molecule; (B) ^{175}Lu content distribution presented as a one-dimensional projection.

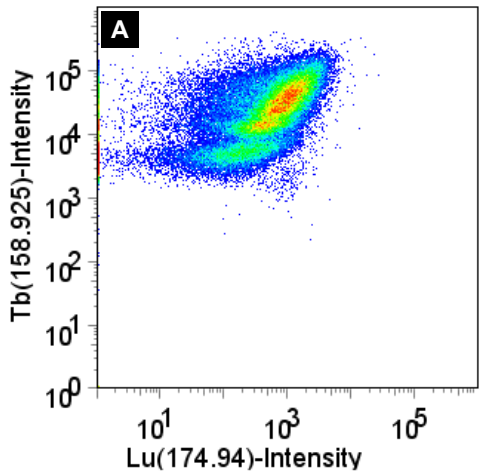

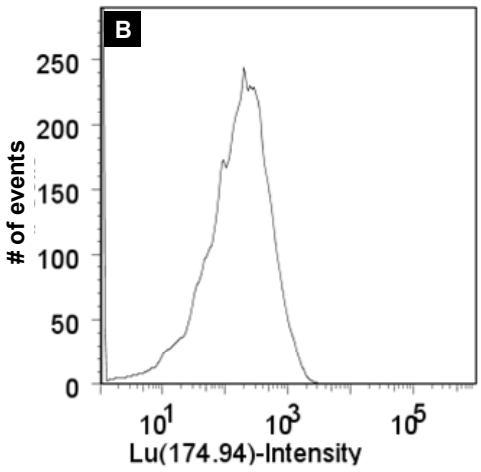

Fig. S19. (A) ^{159}Tb-^{175}Lu isotopic dot-dot diagram for particles from sample ST125 after bioconjugation with Neutravidin and incubation with an Lu-labeled biotin reporter molecule; (B) ^{175}Lu content distribution presented as a one-dimensional projection.

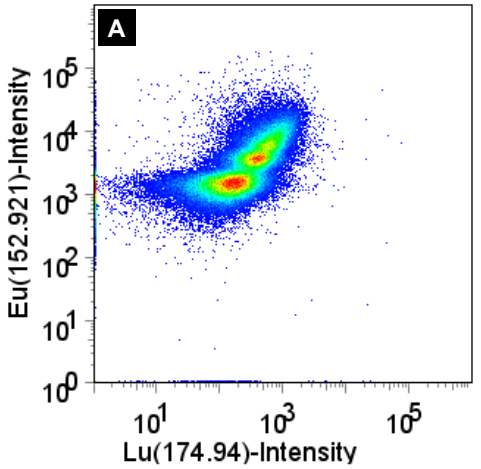

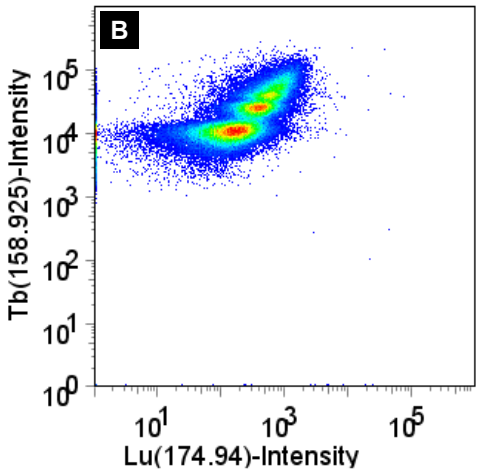

Fig. S20. (A) ^{153}Eu-^{175}Lu isotopic dot-dot diagram for particles from sample ST130 after bioconjugation with Neutravidin and incubation with an Lu-labeled biotin reporter molecule; (B) ^{159}Tb-^{175}Lu isotopic dot-dot diagram from the same sample (note that ST130 was loaded with synthesized with a mixture Eu and Tb complexes to load both metals into the particle interior).

In the Ln content distributions shown above, the variation in intensity on a particle-by-particle basis is very broad. Similar to the results presented in the manuscript, there are detected particle events that differ in the measured Ln content by several orders of magnitude. The measured LnCD also exhibit multimodal character in the case of sample ST130 (Figure S20).

The mean intensities of the Ln in the particle core (Eu, Tb) and the mean intensity of the Lu from the biotin reporter that is bound to Neutravidin for a variety of samples are presented in Table S11. The mean Lu intensity for these samples falls in the range of 10^2 – 10^3. The mean number of Lu per particle is equal to the mean intensity × 550 (the *intensity coefficient* for Lu which is an instrument calibration factor). As each Lu-biotin reporter chelates one metal ion, this means that the number of bound Neutravidin groups per particle varies between 10^4 – 10^5. This number of bound Neutravidin moieties is similar to the value quoted in the manuscript where pre-labeled Neutravidin was used.

Table S11. Mean Ln intensities for metal in particle core and Lu reporter tag from mass cytometry analyses of particles where Neutravidin was covalently bound to the particle surface followed by incubation with an Lu-labeled biotin reporter molecule. The mean number of Lu per particle is equal to the mean intensity multiplied by the *intensity coefficient* (an instrument calibration factor) which is 550 for Lu.

Sample	Particle Label	Mean Ln Intensity	Mean Reporter (Lu) Intensity
ST120	Eu	1472 (^{153}Eu)	932
ST124	Eu	1778 (^{153}Eu)	242
ST125	Tb	5427	218
ST130	Eu	1463 (^{153}Eu)	169
	Tb	10789	
ST154	Eu	3044 (^{153}Eu)	272
ST162	Eu	1298 (^{153}Eu)	412

Notes and references

1. R. G. Gilbert, *Emulsion Polymerisation: A Mechanistic Approach*, Academic Press, San Diego, 1995.
2. M. Morton, S. Kaizerman and M. W. Altier, *Journal of Colloid Science*, 1954, **9**, 300-312.
3. T. Cheikhalard, L. Tighzert and J. P. Pascault, *Die Angewandte Makromolekulare Chemie*, 1998, **256**, 49-59.
4. S. Kawaguchi, A. Yekta and M. A. Winnik, *Journal of Colloid and Interface Science*, 1995, **176**, 362-369.
5. D. E. Koppel, *Journal of Chemical Physics*, 1972, **57**, 4814-4820.